Available online at www.sciencedirect.com
SCIENCE DIRECT®
Journal of Photochemistry and Photobiology A: Chemistry 162 (2004) 97–103
Journal of Photochemistry and Photobiology A:Chemistry
www.elsevier.com/locate/jphotochem

Degradation of amitrole by excitation of iron(III) aquacomplexes in aqueous solutions

Carole Catastini [a], Salah Rafqah [b], Gilles Mailhot [a], Mohamed Sarakha [a,*]

[a] *Laboratoire de Photochimie Moléculaire et Macromoléculaire, Université Blaise Pascal, UMR CNRS 6505, F-63177, Aubière Cedex, France*
[b] *Laboratoire Physico-Chimie des Matériaux, Faculté des Sciences B.P. 45, Université Chouaïb Doukkali El Jadida, El Jadida, Morocco*

Received 27 May 2003; received in revised form 25 June 2003; accepted 27 June 2003

Abstract

The induced degradation of amitrole (3-amino-1,2,4-triazole or aminotriazole) by excitation of iron(III) aquacomplexes was investigated under irradiation at $\lambda = 365$ nm. The process mainly involved the predominant monomeric species of iron(III), namely $Fe(OH)^{2+}$, which leads to the formation of hydroxyl radicals upon excitation in the UV-Vis region. Competitive reactions experiments using nanosecond laser flash photolysis were undertaken for the determination of the second-order rate constant for the reaction of amitrole with hydroxyl radical. A value of $1.5 \times 10^9\ mol^{-1}\,l\,s^{-1}$ was obtained. The quantum yield of amitrole disappearance upon irradiation of the mixture amitrole/iron(III) increased with increasing oxygen concentration and was found to be independent on iron(III) and amitrole concentration. The high performance liquid chromatography (HPLC) analyses showed the formation of two main photoproducts: 5-hydroxy amitrole and urazole (2-aminothiazole). The latter product accumulated in the solution while the former rapidly disappeared with the irradiation time. Efficient mineralisation of the solutions was obtained by artificial as well as by sunlight irradiations.

Keywords: Pesticide; Amitrole; Hydroxyl radical; Iron(III); Photodegradation; Mineralisation

1. Introduction

The photochemical treatment of wastewater containing pesticides may be considered as a good method to destroy recalcitrant pollutants. Various techniques were used and employed for this purpose [1–3]. They mainly involve the formation of hydroxyl radicals, highly reactive species which can oxidize the majority of organic compounds [4]. Its oxidation potential is as high as 2.80 V. These techniques are designated as advanced oxidation processes (AOPs) and they are considered to have considerable potential in this area. In most of the cases, a total mineralisation of contaminated aqueous solutions can be reached.

Iron(III) aquacomplexes absorb a fraction of the available solar light (up to 500 nm) [5]. Therefore, our objective is to explore iron(III)-mediated photodegradation processes of organic pollutants. As largely reported in the literature, the irradiation of iron(III) aquacomplexes leads to the production of hydroxyl radicals by excitation into the ligand to metal charge transfer (LMCT) band [5,6]. This process appeared to be very efficient with $Fe(H_2O)_5(OH)^{2+}$ (represented hereafter by $Fe(OH)^{2+}$) and to significantly depend on the excitation wavelength [5]:

$$Fe(OH)^{2+} \xrightarrow[\text{LMCT}]{h\nu} Fe^{2+} + {}^{\bullet}OH$$

In order to reach the mineralisation of organic pollutants, it was necessary to regenerate iron(III) species in order to permit the production, in a continuous manner, of hydroxyl radicals. Such behaviour was shown to proceed via a homogeneous photocatalytic cycle involving iron(II), iron(III) and oxygen [7]. Several other pathways leading to the regeneration of iron(III) were also taken into account [8]:

$$Fe^{2+} + HO_2^{\bullet} \rightarrow Fe^{3+} + O_2 + H^+$$

$$Fe^{2+} + H_2O_2 \rightarrow Fe^{3+} + {}^{\bullet}OH + {}^{-}OH$$

Because of the low concentration of the implicated species, $HO_2^{\bullet}$ and H_2O_2, these reactions may play a minor role in the degradation process.

This work consists on the photoinduced degradation of the pesticide amitrole (3-amino-1,2,4-triazole or aminotriazole) and represents a continuation of previous studies out of our laboratory. Amitrole is a well-known pesticide which is often used in combination with other active agents in weed control and along roadways and railways [9,10]. It is non-selective

* Corresponding author. Tel.: +33-4-73-40-71-70; fax: +33-4-73-40-77-00.
E-mail address: mohamed.sarakha@univ-bpclermont.fr (M. Sarakha).

1010-6030/$ – see front matter © 2004 Elsevier B.V. All rights reserved.
doi:10.1016/S1010-6030(03)00316-2

and largely employed to substitute some banned herbicides. Because of its low volatility (bp = 260 °C) and good solubility in water (280 g l^{-1}) [11], it can be found in relatively important amount in surface waters and groundwater wells where it has to be removed in order to protect environment. Only few results on the degradation of amitrole are reported. For example, under aerobic conditions, mineralisation represents the main degradation pathway [12,13].

This paper reports on the photochemical degradation and mineralisation of amitrole induced by excitation of iron(III) at 365 nm. Mechanistic details for its disappearance were elucidated by identifying the intermediate photoproducts.

2. Experimental

2.1. Reagents and solutions

$Fe(ClO_4)_3{\cdot}9H_2O$ (97%) was purchased from Fluka and used without further purification. 3-Amino-1,2,4-triazole or amitrole was a Riedel-de Haën product. Urazole (2-aminothiazole) was from Aldrich and was used as received.

Potassium dihydrogenophosphate (KH_2PO_4) and disodium hydrogenophosphate dodecahydrate (Na_2HPO_4) used for the preparation of the buffer for high performance liquid chromatography (HPLC) analyses were Merck products. Acetonitrile was from Carlo Erba (HPLC grade). All other chemicals were of the highest grade available and were used as received. All solutions were prepared with deionised ultrapure water which was purified with Milli-Q device (Millipore) and its purity was controlled by its resistivity (>18 MΩ cm). The deoxygenation of the solutions was accomplished by bubbling argon for 30 min at room temperature. For prolonged irradiations, nitrogen bubbling was maintained during the irradiation. The pH measurements were carried out with a JENWAY 3310 pH-meter to ±0.01 pH unit. The ionic strength was not controlled.

2.2. Irradiations and analysis

The concentration of iron(II) was determined by complexometry with *ortho*-phenanthroline taking $\varepsilon_{510\,nm} = 1.118 \times 10^4\,mol^{-1}\,l\,cm^{-1}$ [14]. By means of the calibration curve, it was carefully checked that no interference in the analysis was observed when amitrole was present in the solution. The concentration of the most photoactive species $[Fe(OH)]^{2+}$, was determined by using 8-hydroxyquinoline-5-sulfonic acid (HQSA) according to the published procedure [15]. The absorbance of the complex $Fe(HQSA)_3$ was taken at λ = 572 nm ($\varepsilon_{572\,nm} = 5000\,mol^{-1}\,l\,cm^{-1}$). The molar fraction of $Fe(OH)^{2+}$ was expressed as the ratio $[Fe(OH)^{2+}]/[iron(III)]_{total}$.

The degradation of amitrole and the formation of urazole were followed by high performance liquid chromatography using a Hewlett-Packard system (HP1050) equipped with a mono-channel UV-Vis detector and an automatic injector. The experiments were performed by UV detection at 230 nm and by using a reverse phase Merck column (Spherisorb ODS 25 μm; 250–4.6 mm). The flow rate was 1 ml min^{-1} and the injected volume was 50 μl. The elution was accomplished with water (pH = 6 using phosphate buffer) and acetonitrile (9.5/0.5 v/v). A Waters 540 HPLC chromatograph equipped with a Waters 996 photodiode array detector was used for obtaining the UV-Vis spectra of the photoproducts.

The progress of the mineralisation of amitrole was monitored by measuring the total organic carbon (TOC) via a Shimadzu Model TOC-5050A equipped with an automatic sample injector. The calibration curve within the range 1–15 mg l^{-1} was obtained by using potassium hydrogen phthalate and sodium hydrogen carbonate for organic and inorganic carbon, respectively.

The progress of ammonia ions formation was obtained either by capillary electrophoresis (Waters Quanta 400) or by ionic chromatography using a Gilson 305 pump equipped with a Waters 431 conductivity detector and a Hamilton cationic column (PRP-X200). The elution was accomplished by using HNO_3 (2.0×10^{-3} M)/methanol (7/3 v/v). The flow was 1.0 ml min^{-1}.

UV-Vis spectra were recorded with a Cary 3 double beam spectrophotometer.

2.3. Time resolved transient absorption

Transient absorption experiments in the 20 ns to 400 μs time scale were carried out on a nanosecond laser flash photolysis spectrometer from Applied Photophysics (LKS60). Excitation (λ = 355 nm) was from the third harmonic of a Quanta Ray GCR 130-01 Nd:YAG laser (pulse width ≈ 5 ns), and was used in a right-angle geometry with respect to the monitoring light beam. A 3 cm^3 volume of solution was used in a quartz cuvette, and was stirred after each flash irradiation. Individual cuvette samples were used for a maximum of three consecutive laser shots. The transient absorbance at preselected wavelength was monitored by a detection system consisting of a pulsed xenon lamp (150 W), monochromator and a photomultiplier (1P28). A spectrometer control unit was used for synchronizing the pulsed light source and programmable shutters with the laser output. This also housed the high-voltage power supply for the photomultiplier. The signal from the photomultiplier was digitized by a programmable digital oscilloscope (HP54522A). A 32 bits RISC-processor kinetic spectrometer workstation was used to analyse the digitized signal.

2.4. Steady-state irradiations

For the determination of the quantum yields, solutions were irradiated at 365 nm in a parallel beam obtained from a Schoeffel monochromator equipped with a xenon lamp (1600 W). The reactor was a quartz cell of 1 cm path length.

The photon flow was evaluated by means of classical ferrioxalate actinometry [14].

For analytical experiments a system consisting of a three lamps (Philips HPW 125 W) giving a main emission at 365 nm (87.5%) together with 313 nm (2.0%), 334 nm (6.5%), 405 nm (2.7%), 434 nm (1.3%) was used. They were symmetrically installed in a stainless steel cylinder (diameter = 33 cm). The reactor, a water-jacketed pyrex tube ($d = 2.8$ cm and $\lambda > 320$ nm) was located in the centre. The solution (100 ml) was stirred during irradiation to insure its homogeneity.

Sunlight photolysis were performed in Clermont-Ferrand on June sunny days (latitude 46°N, 420 m above sea level) in pyrex tube (39 cm long and 3.5 cm diameter with 2 mm thickness, $\lambda > 320$ nm). The sunlight intensity was not measured.

3. Results and discussion

Amitrole ($pK_{a1} = 4.2$ and $pK_{a2} = 10.7$ [16]) absorbs significantly in the ultraviolet region at $\lambda < 250$ nm (Fig. 1). Upon excitation at 365 nm, no disappearance of amitrole was observed. It is worth noting that the absorption spectra of mixtures of iron(III) (3.0×10^{-4} mol l^{-1}) with amitrole (1.0×10^{-4} mol l^{-1}), pH = 3.3, were shown to be equal to the sum of the component spectra. This clearly indicates that under the conditions of our experiments, no significant ground state interaction between iron(III) and amitrole was present. As shown in Fig. 1, the mixture iron(III)/amitrole presents a UV absorption spectrum which extends to approximately 500 nm, due to the presence of iron(III) species. An important overlap is observed with the solar emission [17].

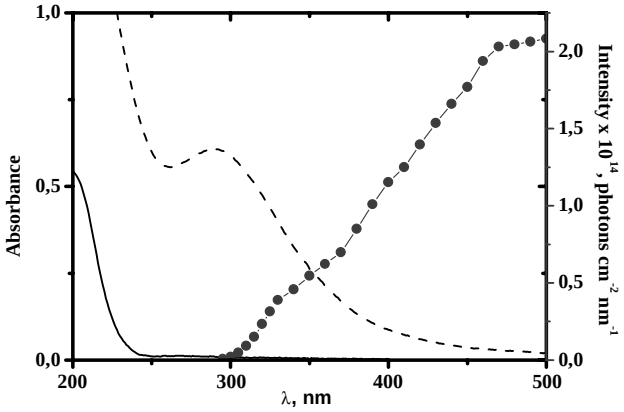

Fig. 1. UV absorption spectra of amitrole (—) 1.0×10^{-4}, mixture amitrole (- - -) 1.0×10^{-4} M/Fe(OH)$^{2+}$ (3.0×10^{-4} M) and sunlight emission (●).

As largely reported in the literature, the monomeric iron(III) species, Fe(OH)$^{2+}$, is the predominant species when the following conditions are used: [iron(III)] = 3.0×10^{-4} mol l^{-1} and pH = 3.4 [5,6,15,18–20]. Its molar fraction was shown to decrease with the ageing of the solution [21]. The disappearance of Fe(OH)$^{2+}$ was attributed to the possible formation of soluble aggregates. For this reason, the quantum yield of amitrole disappearance and that of iron(II) formation were determined for different molar fraction of Fe(OH)$^{2+}$.

3.1. Effect of Fe(OH)$^{2+}$ molar fraction

As shown in Table 1, the quantum yields of amitrole degradation and iron(II) formation decreased when the molar fraction of Fe(OH)$^{2+}$ decreased. They were calculated by using the total absorbance of the solution at the excitation wavelength (365 nm). As already reported in the literature, such absorbance is due to the presence of various species of iron(III) which do not have equivalent photoreactivities [21]. The quantum yields were corrected by taking into account the absorbance of Fe(OH)$^{2+}$ calculated by using the molar absorption coefficient ($\varepsilon_{365\,nm} = 220$ mol^{-1} l cm^{-1}) [5,15,22,23]. The following correction was used:

$$\Phi_i^c = \Phi_i \left(\frac{A_{solution}}{A_{FeOH^{2+}}} \right)$$

where Φ_i^c is the corrected quantum yield, $A_{solution}$ and $A_{Fe(OH)^{2+}}$ represent the absorbances of the solution and of Fe(OH)$^{2+}$, respectively. As shown in Table 1, the quantum yields appeared, within the experimental errors, to be constant when the molar fraction of the monomeric species decreased. This result indicates that the disappearance of amitrole as well as the formation of iron(II) are only due to the excitation of Fe(OH)$^{2+}$. This is in good agreement with the fact that such species is the most photoactive species under our experimental conditions. Moreover, the values reported in Table 1 also show that the ratio $\Phi^c_{iron(II)}/\Phi^c_{amitrol}$

Table 1
Quantum yields of amitrole disappearance and iron(II) formation as a function of Fe(OH)$^{2+}$ molar fraction

$x_{Fe(OH)^{2+}}$	$\Phi_{amitrole}$	$\Phi_{iron(II)}$	$\Phi_{camitrole}$	$\Phi_{ciron(II)}$	$\Phi^c_{iron(II)}/\Phi^c_{amitrol}$
0.90	4.1×10^{-3}	3.8×10^{-2}	4.4×10^{-3}	4.1×10^{-2}	9.3
0.75	3.5×10^{-3}	3.2×10^{-2}	4.1×10^{-3}	3.7×10^{-2}	9.0
0.50	1.8×10^{-3}	1.7×10^{-2}	4.2×10^{-3}	4.0×10^{-2}	9.5
0.40	1.6×10^{-3}	1.5×10^{-2}	3.9×10^{-3}	3.7×10^{-2}	9.5
0.20	1.0×10^{-3}	9.0×10^{-3}	4.2×10^{-3}	3.8×10^{-2}	9.0
0.10	7.0×10^{-4}	6.5×10^{-3}	3.9×10^{-3}	3.6×10^{-2}	9.2

[Amitrole] = 1.0×10^{-4} M, pH = 3.4, $\lambda_{excitation} = 365$ nm, aerated solution.

Table 2
Quantum yields of amitrole disappearance and iron(II) formation in aerated aqueous solutions as a function of iron(III) concentration

[iron(III)] (M)	$\Phi_{amitrole}$	$\Phi_{iron(II)}$
2.0×10^{-5}	1.9×10^{-3}	1.9×10^{-2}
5.0×10^{-5}	1.9×10^{-3}	1.7×10^{-2}
1.0×10^{-4}	1.8×10^{-3}	1.7×10^{-2}
2.0×10^{-4}	1.7×10^{-3}	1.8×10^{-2}
5.0×10^{-4}	1.8×10^{-3}	1.6×10^{-2}
1.0×10^{-3}	1.6×10^{-3}	1.7×10^{-2}

[Amitrole] = 1.0×10^{-4} M, pH = 3.4, $\lambda_{excitation}$ = 365 nm, $x_{Fe(OH)^{2+}} \approx 0.5$.

is constant and roughly equal to 9. Additional pathways for the formation of iron(II) must then be taken into account in the degradation process of the organic substrate. No effect of the initial concentration of amitrole was observed within the range 5.0×10^{-5} to 1.0×10^{-2} mol l^{-1}. Such behaviour excludes the possibility of interaction between iron(III) in its excited state and amitrole as reported with 2,6-dimethylphenol [24].

3.2. Effect of iron(III) initial concentration

This effect was studied at a constant molar fraction of the monomeric species $Fe(OH)^{2+}$, $x_{Fe(OH)^{2+}} \approx 0.5$. As reported in Table 2, the quantum yields are constant within the concentration range 2.0×10^{-5} to 1.0×10^{-3} mol l^{-1}. It also shows that the disappearance of amitrole was efficient at low concentration of iron(III). Two different pathways can then be proposed for the photochemical degradation of amitrole.

3.3. Effect of oxygen concentration

The molecular oxygen most often plays an important role in the photochemical degradation of organic pollutants. As shown in Table 3, the disappearance of amitrole induced by excitation of iron(III) decreased when the oxygen concentration decreased. A factor of 4 is observed when the experiments were undertaken in deoxygenated and oxygenated solutions. It is worth noting that the disappearance is not completely inhibited in the absence of oxygen.

Table 3
Effect of oxygen concentration on the quantum yields of amitrole disappearance and iron(II) formation

Conditions	[Oxygen] (M) [25]	$\Phi_{amitrole}$	$\Phi_{fer(II)}$
Deaerated	$<10^{-5}$	1.0×10^{-3}	2.1×10^{-2}
Aerated	2.64×10^{-4}	3.5×10^{-3}	3.2×10^{-2}
Oxygenated	1.29×10^{-3}	3.8×10^{-3}	3.3×10^{-2}

[Amitrole] = 1.0×10^{-4} M, [iron(III)] = 3.0×10^{-4} M, $x_{Fe(OH)^{2+}} \approx 0.75$, pH = 3.4.

3.4. Effect of 2-propanol

The photoreactivity of the monomeric species $Fe(OH)^{2+}$ mainly involves the formation of hydroxyl radicals. They can be easily trapped by adding 2-propanol in the solution [4,26,27]. In the presence of such alcohol at a concentration as high as 0.10 mol l^{-1} and in aerated solution, the disappearance of amitrole was completely inhibited. The degradation is then totally due to the attack of hydroxyl radicals.

3.5. Laser flash photolysis studies

To establish the mechanism and kinetic details of amitrole degradation photoinduced by $Fe(OH)^{2+}$, we employed a nanosecond laser flash photolysis technique. No transient was observed within the range 300–500 nm when a mixture amitrole (1.0×10^{-4} mol l^{-1}) and iron(III) (2.0×10^{-3} mol l^{-1}) at $x_{Fe(OH)^{2+}} \approx 0.9$, was excited at 355 nm. The transient formed by the reaction with the hydroxyl radical most likely absorbs at lower wavelengths. In order to determine the absolute rate constant for this reaction, a competitive reactions method using sulfanilamide and amitrole was undertaken:

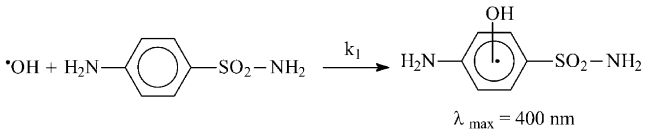

(1)

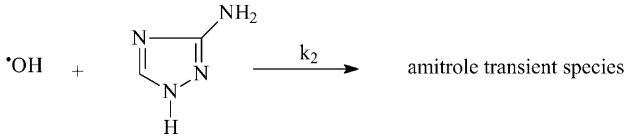

(2)

Eq. (1) is reported in the literature and the rate constant k_1 was found to be equal to 6.7×10^9 mol^{-1} l s^{-1} [28]. The process leads to the formation of a radical species which was assigned to the adduct •OH-sulfanilamide. Under these conditions, the rate constant for the oxidation process of amitrole (Eq. (2)) may be determined by following the growth of the absorbance of such adduct. The overall rate law my be expressed as follows:

$$\frac{d[^{\bullet}\text{OH-sulfanilamide}]}{dt} = k_{obs}[^{\bullet}\text{OH}]$$

where k_{obs} is the observed pseudo first-order rate constant:

$$k_{obs} = k_2[\text{amitrole}] + k_1[\text{sulfanilamide}]$$

Aqueous solutions of sulfanilamide (1.0×10^{-4} mol l^{-1}) and iron(III) (2.0×10^{-3} mol l^{-1}, $x_{Fe(OH)^{2+}} \approx 0.9$) were studied by laser flash photolysis at various concentrations of amitrole (within the range 1.5×10^{-4} to 7.7×10^{-4} mol l^{-1}).

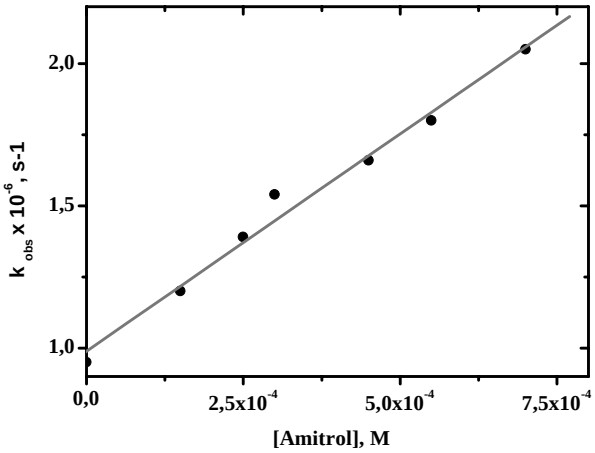

Fig. 2. The pseudo first-order rate constant for the formation of the adduct •OH-sulfanilamide at 400 nm as a function of amitrole concentration. [Sulfanilamide] = 1.0×10^{-4} M, [iron(III)] = 3.0×10^{-4} M, $x_{Fe(OH)^{2+}} \approx 0.9$, pH = 3.4.

The pseudo first-order constant, k_{obs}, was determined by analysing the build-up at 400 nm corresponding to the formation of •OH-sulfanilamide species. As shown in Fig. 2, a linear plot was obtained when k_{obs} is expressed as a function of amitrole concentration. The value 1.5×10^9 mol^{-1} l s^{-1} was obtained for k_2 from the slope.

3.6. Photoproducts analysis

The photolysis at 365 nm of aqueous solutions of amitrole (1.0×10^{-4} mol l^{-1}) in the presence of iron(III) (3.0×10^{-4} mol l^{-1}, $x_{Fe(OH)^{2+}} \approx 0.9$) led to a continuous increase of the absorbance over the whole UV-Vis absorption spectrum. The HPLC analyses of the irradiated solution gave a clear evidence for the formation of two main products (Fig. 3). The product at $t_{retention} = 3.0$ min, urazole, was easily identified by comparison of its retention time and UV-Vis spectrum with those of an authentic sample.

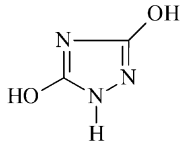

Urazole

Urazole which accumulates in the solution cannot be formed as a primary product. As shown in Fig. 3, its formation was only observed after 3 min irradiation time while product **I** ($t_{retention} = 2.6$ min) appeared from the early stages of the irradiation. **I** disappeared in its turn after 20 min irradiation time (Fig. 4). As indicated in Fig. 4, **I** appeared to be the precursor of urazole. **I** may be assigned to a monohydroxylated product: 5-hydroxy amitrole or 3-hydroxy triazole.

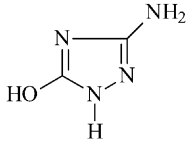

5-hydroxy amitrole

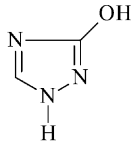

3-hydroxy triazole

All the attempts to detect ammonia ions by capillary electrophoresis and cationic chromatography in the early irradiation time failed. This result indicates that 3-hydroxy triazole was not formed under our experimental conditions and only 5-hydroxy amitrole may be obtained as a primary photoproduct.

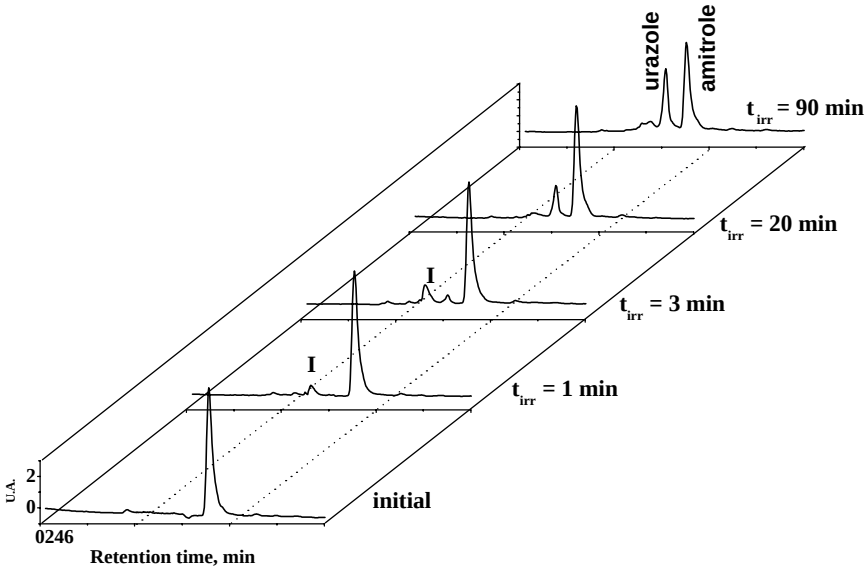

Fig. 3. High performance liquid chromatogram observed for the products of photolysis of aerated aqueous solutions of iron(III) (3.0×10^{-4} M), $x_{Fe(OH)^{2+}} \approx 0.9$ in the presence of amitrole (1.0×10^{-4} M), $\lambda_{excitation} = 365$ nm, pH = 3.4.

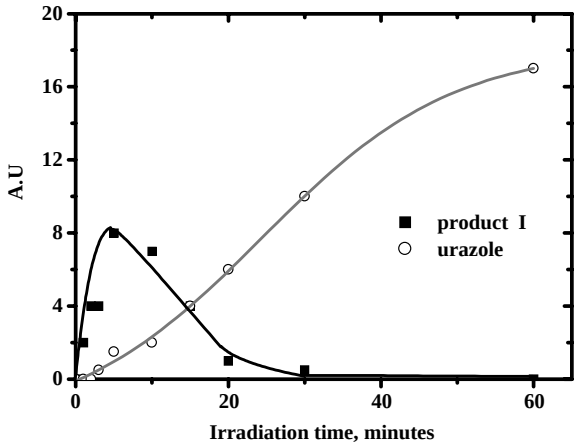

Fig. 4. Evolution of the photoproducts **I** and urazole as a function of irradiation time in aerated aqueous solution. $\lambda_{excitation} = 365\,nm$, [amitrole] $= 1.0 \times 10^{-4}$ M, [iron(III)] $= 3.0 \times 10^{-4}$ M, $x_{Fe(OH)^{2+}} \approx 0.9$, pH $= 3.4$.

The two photoproducts, urazole and 5-hydroxy amitrole, were also observed when the experiments were carried out in deoxygenated solutions. Under these conditions, their formation rates were lower by a factor of 2 than those obtained in aerated solutions.

3.7. Mechanism

As clearly demonstrated by the inhibition of the reaction by 2-propanol and also by nanosecond laser flash photolysis experiments, hydroxyl radicals are the key species in the degradation process of amitrole. Their formation involves the excitation of $Fe(OH)^{2+}$ into the ligand to metal charge transfer band [5,6]. The oxidation of amitrole by hydroxyl radicals may lead to the formation of the adduct •OH-amitrole: a reaction similar to that generally observed with aromatic derivatives [28–30].

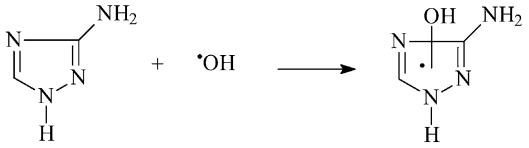

In the presence of oxygen, the evolution of the adduct •OH-amitrole to form 5-hydroxy amitrole may be represented by the following reactions:

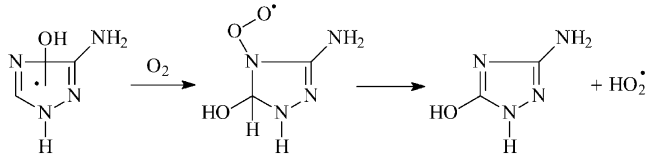

The disappearance of the adduct •OH-amitrole may also involve ferric ions leading to the formation of iron(II) and to 5-hydroxy amitrole:

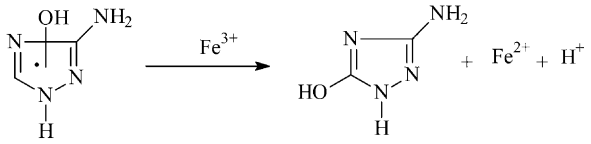

Such process which can be observed in the presence as well as in the absence of oxygen, represents an additional pathway for the formation of iron(II). This is in good agreement with the fact that the quantum yield of iron(II) formation is higher than that of amitrole disappearance.

The formation of urazole, as a secondary product, may be explained by the reactivity of the hydroxyl radical with 5-hydroxy amitrole leading to the formation of an equivalent amount of ammonia ions. A process similar to that proposed above for amitrole.

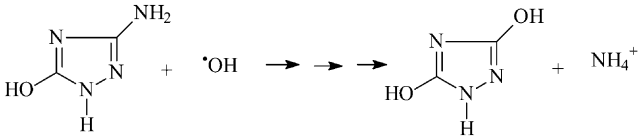

3.8. Total degradation of amitrole and mineralisation

Irradiation of the mixture amitrole ($1.0 \times 10^{-4}\,mol\,l^{-1}$)/iron(III) ($3.0 \times 10^{-4}\,mol\,l^{-1}$, $x_{Fe(OH)^{2+}} \approx 0.9$) was carried at pH $= 3.4$ and in aerated conditions. In Fig. 5 are presented the disappearance of amitrole and the formation of iron(II) species. It clearly shows that the total degradation of amitrole was observed after about 650 min irradiation time. In the meantime, the concentration of iron(II) rapidly increased and reached a limit value at approximately $2.7 \times 10^{-4}\,mol\,l^{-1}$. This result indicates the complete disappearance of the starting $Fe(OH)^{2+}$ species. In the absence of oxygen, only 25% conversion of amitrole was observed.

The progress of the mineralisation of the solution was monitored by measuring the total organic carbon. As shown

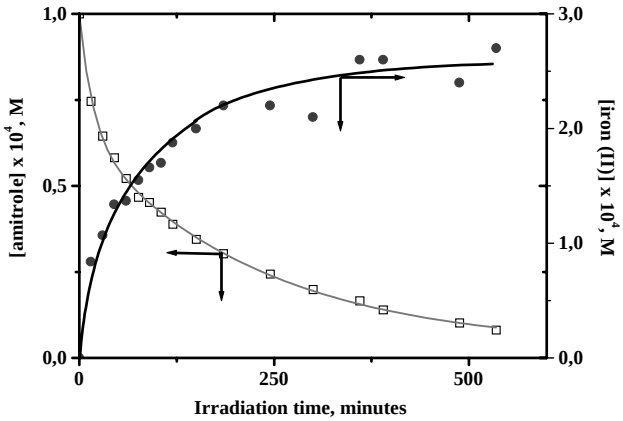

Fig. 5. Degradation of amitrole and iron(II) formation upon irradiation of iron(III) (3.0×10^{-4} M)/amitrole (1.0×10^{-4} M) mixture at 365 nm in aerated solution, $x_{Fe(OH)^{2+}} \approx 0.9$, pH $= 3.4$.

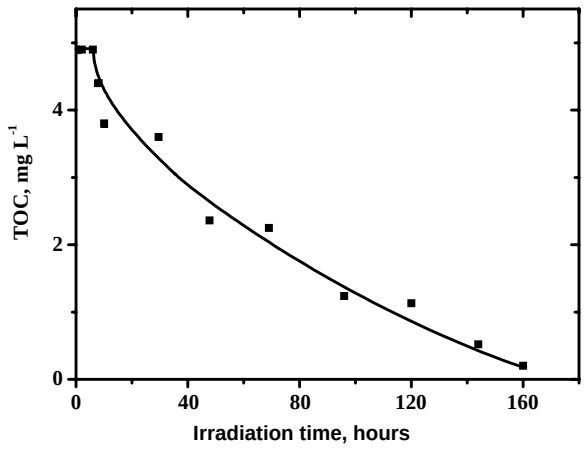

Fig. 6. Time evolution of the total organic carbon (TOC) values during irradiation of iron(III) (3.0×10^{-4} M)/amitrole (2.0×10^{-4} M) mixture at 365 nm, pH = 3.4.

in Fig. 6, the mineralisation of 2.0×10^{-4} mol l^{-1} of amitrole appeared after 10 h irradiation time. The lag period of about 5 h corresponds to a period within which urazole and other photoproducts accumulate in the solution. The generated photoproducts are attacked in their turn by hydroxyl radicals which are formed in a continuous manner via a homogeneous photocatalytic process involving iron(III), iron(II) and oxygen [7]. The progress of the ammonia ions as a function of irradiation time is presented in Fig. 7. It is in good agreement with an efficient mineralisation of amitrole solutions. It is of interest to note that the total degradation of amitrole and also its mineralisation are also observed when solar light was used for excitation.

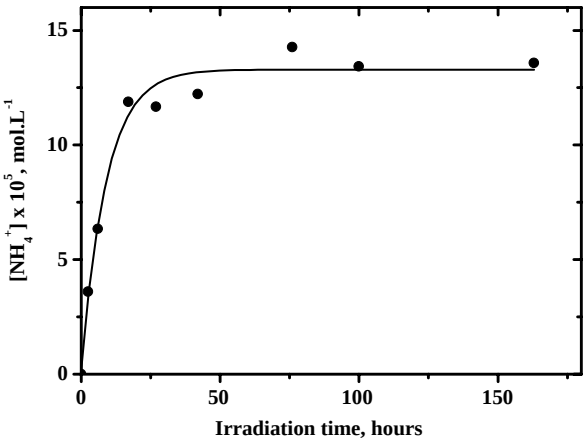

Fig. 7. Time evolution of the ammonia ions concentration during irradiation of iron(III) (3.0×10^{-4} M)/amitrole (1.0×10^{-4} M) mixture at 365 nm, pH = 3.4.

4. Conclusion

The degradation of amitrole by excitation of $Fe(OH)^{2+}$ has been reported to be very efficient. The mechanism of photoinduced degradation involves only the attack by hydroxyl radicals. The major product was found to be urazole which is formed via the initial production of 5-hydroxy amitrole. Under the experimental conditions, the total degradation was obtained after 10 h irradiation time while mineralisation of the solution was attained after 160 h.

References

[1] O. Legrini, E. Oliveros, A.M. Braun, Chem. Rev. 93 (1993) 671–698.
[2] D.F. Ollis, H. Al-Ekabi (Eds.), Photocatalytic Purification of Water and Air, Elsevier, Amsterdam, 1993.
[3] R.G.W. Norrish, F.R.S. Wayne, R.P. Wayne, Proc. R. Soc. London, Ser. A 228 (1965) 361–370.
[4] G.V. Buxton, C.L. Greenstock, W.P. Helman, A.P. Ross, J. Phys. Chem. 17 (1988) 513–886.
[5] H.-J. Benkelberg, P. Warneck, J. Phys. Chem. 99 (1995) 5214–5221.
[6] P. Mazellier, M. Sarakha, M. Bolte, New J. Chem. (1999) 133–135.
[7] C. Catastini, M. Sarakha, G. Mailhot, M. Bolte, Sci. Total Environ. 298 (2002) 219–228.
[8] B.H. Bielski, D.E. Cabelli, R.L. Arudi, J. Phys. Chem. 14 (1985) 1041–1100.
[9] M. Ersoz, H.J. Duncan, M. Lale, H.I. Ucan, Environ. Technol. 17 (1996) 87.
[10] L. Agnolucci, F.D. Vecchia, R. Barbato, V. Tassani, G. Casadoro, N. Rascio, J. Plant. Physiol. 147 (1996) 493.
[11] H. Kidd, D.R. Jones, The Agrochemicals Handbook, third ed., Royal Society of Chemistry, Cambridge, 1991.
[12] T. Oesterreich, U. Klaus, M. Volk, B. Neidhard, M. Spiteller, Chemosphere 38 (1999) 379.
[13] U. Klaus, T. Oesterreich, M. Volk, M. Spiteller, Acta Hydrochim. Hydrobiol. 26 (1998) 311.
[14] J.G. Calvert, J.M. Pitts, Photochemistry, Wiley, New York (1996) 783–786.
[15] B.C. Faust, J. Hoigné, Atmos. Environ. 24A (1990) 79–89.
[16] V. Pichon, M.C. Hennion, Anal. Chim. Acta 284 (1993) 317.
[17] R. Franck, W. Klöpffer, Chemosphere 17 (1988) 985–994.
[18] N. Brand, G. Mailhot, M. Bolte, J. Environ. Sci. Technol. 32 (1998) 2715–2720.
[19] P. Mazellier, J. Jirkovsky, M. Bolte, Pestic. Sci. 49 (1997) 259–267.
[20] C.H. Langford, J.H. Carey, Can. J. Chem. 53 (1975) 2430.
[21] C.M. Flynn, Chem. Rev. 54 (1984) 31–41.
[22] R.J. Knight, R.N. Sylva, J. Inorg. Nucl. Chem. 37 (1975) 779.
[23] R.N. Sylva, Rev. Pure Appl. Chem. 22 (1972) 115.
[24] P. Mazellier, G. Mailhot, M. Bolte, New J. Chem. 21 (1997) 389–397.
[25] S.L. Murov, I. Carmichael, G.L. Hug, Handbook of Phtochemistry, second ed., Marcel Dekker, New York, 1993, p. 293.
[26] Y. Sun, J. Pignatello, Environ. Sci. Technol. 27 (1993) 304–310.
[27] W.H. Glaze, Environ. Sci. Technol. 21 (1987) 224–230.
[28] S.P. Ramnani, S. Dhanya, P.K. Bhattacharyya, Radiat. Phys. Chem. 50 (3) (1997) 277–282.
[29] D. Behar, B. Behar, J. Phys. Chem. 95 (1991) 7552–7556.
[30] U. Stafford, K.A. Gray, P.V. Kamat, J. Phys. Chem. 98 (1994) 6343.